

ment to neutron diffraction techniques applied to transformations in which soft-mode behavior is suspected.

As for the ω phase in ZrNb it can be definitely concluded that there are dynamical aspects to the instability towards the formation of the ω phase. The diffuse scattering could not result solely from static distributions of small ω -phase particles. One can only speculate on the source of the inelastic scattering. One possibility is that local regions of the bcc matrix fluctuate so that the atomic configuration resembles the hexagonal ω phase, and that in time this dissolves away and the hexagonal-like fluctuation appears in another region of the crystal.

Another possibility is that hexagonal-like regions behave as very small crystallites which have the vibrational modes of a relatively large unit, and it is scattering from this vibrating unit

that results in inelastic scattering.

We are particularly indebted to Professor S. Sass for providing the specimens, and to Dr. D. Keating for helpful discussion. One of us (B.W.B.) wishes to express his gratitude to the John Simon Guggenheim Foundation for supporting this work.

*Work supported by a grant from the John Simon Guggenheim Foundation. Permanent address: Department of Materials Science and Engineering, Cornell University, Ithaca, N.Y. 14850.

¹C. Ghezzi, A. Merlini, and S. Pace, *Nuovo Cimento* **64B**, 103 (1969).

²G. Albanese, C. Ghezzi, A. Merlini, and S. Pace, *Phys. Rev. B* **5**, 1745 (1972).

³S. C. Moss, D. T. Keating, and J. D. Axe, *Bull. Amer. Phys. Soc.* **18**, 313 (1972).

⁴S. Sass, *J. Less-Common Metals* **28**, 157 (1972).

Interband Masses of Higher Interband Critical Points in Ge

D. E. Aspnes

Bell Laboratories, Murray Hill, New Jersey 07974

(Received 15 May 1973)

Interband reduced masses for the critical points E_0 , $E_0 + \Delta_0$, E_1 , $E_1 + \Delta_1$, E_0' , $E_0' + \Delta_0'$, $E_0' + \Delta_0' + \Delta_0$, and E_2 have been determined accurately for Ge from Franz-Keldysh oscillations. The observation of a well-defined interband reduced mass for the E_2 structure suggests a relatively well-localized critical-point origin for this spectral feature, in contrast to presently accepted interpretations.

Although effective masses contain information about exchange and correlation effects¹ in addition to mutual interactions between bands well separated in energy, these parameters are generally neglected in energy-band theory principally because, with very few exceptions,^{2,3} it has not been possible to obtain any direct information about them except in the vicinity of fundamental direct or indirect absorption edges. In this Letter, we report the first experimental measurement, for any material, of the interband reduced masses for a complete set of direct interband critical points up to and including the E_2 transition. In addition to demonstrating that reduced masses of higher interband critical points are accessible to experimental investigation, these new results show that the E_2 critical point in Ge has a well-defined interband reduced mass, which indicates a relatively well-localized contributing region in contrast to presently accepted interpre-

tations for this spectral feature in Ge and in other semiconductors.³⁻⁸

Interband reduced masses are determined here by means of subsidiary or Franz-Keldysh oscillations⁹ which arise in the theory of electroreflectance (ER). These oscillations are not present in the low-field theory usually applicable to higher-interband transitions, but must be described mathematically by intermediate-field theory¹⁰ which predicts

$$\frac{\Delta R}{R} \sim C_1(E) + \operatorname{Re} \left\{ C_2(E) e^{-Q(E)} \cos \left[\frac{2}{3} \left(\frac{E - E_s}{\hbar \Omega} \right)^{3/2} + \theta_0 \right] \right\}. \quad (1)$$

Here, $\Delta R/R = [R(\mathcal{E}_s) - R(0)]/R(0)$ is the usual modulated relative reflectance spectrum measured in ER; \mathcal{E}_s is the surface field; and $C_1(E)$, $C_2(E)$, $Q(E)$, and θ_0 are coefficients which vary slowly

with energy on the scale of the argument of the cosine term and need not be considered further. The interband reduced mass in the field direction, μ_{\parallel} , enters through the characteristic energy $\hbar\Omega$, defined by

$$(\hbar\Omega)^3 = e^2 \mathcal{E}_s \hbar^2 / 8\mu_{\parallel}. \quad (2)$$

Therefore, the period of the oscillations can be used to determine μ_{\parallel} .¹¹

Franz-Keldysh oscillations are well known at fundamental absorption edges,¹¹⁻¹³ where the intrinsic broadening Γ is sufficiently small so that the intermediate-field condition ($\hbar\Omega > \Gamma/3$) is easily obtained. We have found that it is also possible to achieve the necessary combination of small broadening parameters and high fields required to make these oscillations observable in higher-interband spectra by making ER measurements at low temperature using the Schottky barrier configuration.^{3,14} Typical data are shown in Fig. 1. These spectra were taken on the [110] face of an *n*-type Ge crystal of net low-temperature carrier concentration $N_D = 6.4 \times 10^{15} \text{ cm}^{-3}$ using a semitransparent Ni film to form the Schottky barrier. The surface-field values were chosen to optimize the oscillations for display purposes. In some cases, e.g., for $E_1 + \Delta_1$ and $E_0' + \Delta_0' + \Delta_0$, the baseline is seen to shift upward with energy

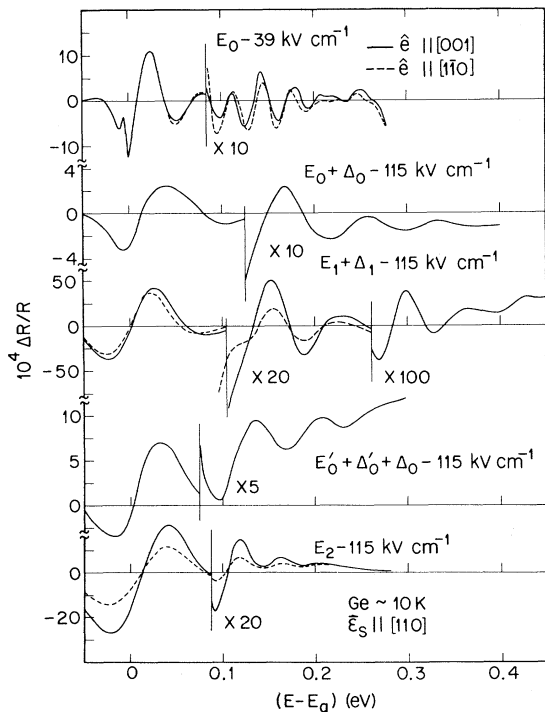


FIG. 1. Representative Franz-Keldysh oscillation spectra observed at various critical points in Ge.

because of the overlap with the low-energy structure of the next higher transition. Polarization effects are also shown where appropriate. These effects appear most prominently in the Franz-Keldysh oscillations at 0.11 and 0.21 eV in the E_0 transition spectrum, due to interference between light- and heavy-hole spectra,¹³ and also at 0.12 eV in the $E_1 + \Delta_1$ spectrum, where the interference now occurs between the two formerly equivalent subgroups of the eight $\langle 111 \rangle$ critical points making different angles with the field. Note particularly the existence of a series of well-defined oscillations extending above the main structure of the E_2 transition.

Interband reduced masses were determined from these and similar data via a simple two-step process. First, the points at which the oscillations in Fig. 1 are tangent to their envelopes (both positive and negative) for each spectrum are numbered consecutively ($\nu = 1, 2, \dots$), the energy difference $E_\nu - E_g$ obtained for each, and $(E_\nu - E_g)^{3/2}$ plotted as a function of ν . This is more accurate than using zero crossings¹³ when the baseline is varying. By Eq. (1), this procedure should yield a straight line of slope $S = 3\pi e \times \mathcal{E}_s \hbar / 4(2\mu_{\parallel})^{1/2}$ for each spectrum. We show in Fig. 2 that the results obtained for a number of representative spectra indeed verify this step. In the second part of the analysis, the Schottky-barrier relation $\mathcal{E}_s^2 \sim V_B - V_{\text{ext}}$ (where V_B is the internal barrier potential and $V_{\text{ext}} < 0$ is the externally applied potential) is used to eliminate \mathcal{E}_s . The barrier relation shows that a plot of S^2 versus V_{ext} , for any single critical point, will also yield a straight line with slope inversely proportional to μ_{\parallel} . This prediction is verified by the results shown in Fig. 3. This second step

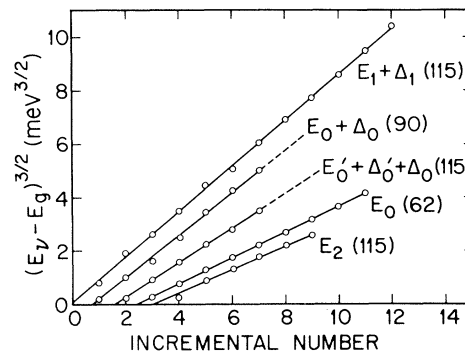


FIG. 2. Plot of tangential energy to the three-halves power versus tangent-point number. The curves have been displaced along the abscissa for display purposes since only the slope is relevant.

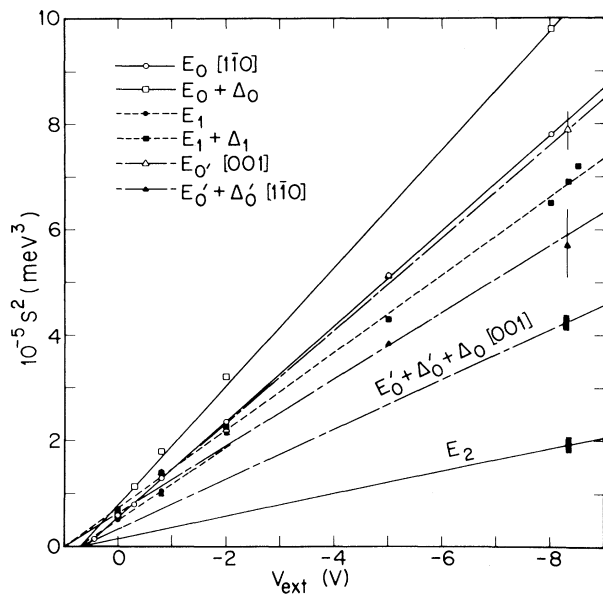


FIG. 3. Plot of square of slope, calculated as shown in Fig. 2, versus external modulation potential at which spectrum was measured. Slopes of the straight lines are inversely proportional to interband reduced masses of the various critical points.

greatly improves the accuracy of determining the interband reduced masses (a) by modifying the dependence of slope on mass from $\mu_{\parallel}^{-1/2}$ to μ_{\parallel}^{-1} , thus improving the functional dependence of the parameter to be determined; (b) by eliminating the accuracy-limiting step of determining \mathcal{E}_s directly for each spectrum; and (c) by providing a consistency check on experiment as well as theory.

Highly accurate *relative* values of μ_{\parallel} can now be obtained between any two critical points from Fig. 3. Accurate absolute values were obtained by choosing the net donor concentration N_D (the remaining parameter after \mathcal{E}_s^2 is eliminated by the barrier equation) to bring μ_{s0} , the isotropic mass of the $E_0 + \Delta_0$ critical point, into agreement with the known value.¹⁵ Absolute values of the interband reduced masses so determined for the eight critical points through E_2 are given in Table I and compared to theoretical values where available. It should be noted that the heavy-hole mass of the fundamental direct edge agrees within 2% of the known value.¹⁵ This result lends further confidence to the procedure, and also indicates

TABLE I. Experimentally determined interband reduced-mass values for critical points in Ge.

Transition	E_g (meV) ^a	Mass component (field [110])	Expt. value ^b (in m_e)	Theor. value
E_0	887.2 ± 1	$\mu_{hh}, \hat{e} [1\bar{1}0]$	0.0336 ± 0.013	0.0343^c
$E_0 + \Delta_0$	1184 ± 2	μ_{s0}	0.0269	0.0269^c
E_1	2250 ± 2	μ_T	0.045 ± 0.004	0.049^d
$E_1 + \Delta_1$	2434 ± 2	μ_T	0.042 ± 0.005	0.050^d
E_0'	3006 ± 5	$\mu, \hat{e} [001]$	0.034 ± 0.005	-
$E_0' + \Delta_0'$	3206 ± 5	$\mu, \hat{e} [1\bar{1}0]$	0.048 ± 0.009	-
$E_0' + \Delta_0' + \Delta_0$	3502 ± 5	$\mu, \hat{e} [001]$	0.062 ± 0.006	-
E_2	4501	$\mu_T(?)$	0.139 ± 0.015	$(0.12)^e$

^aCritical point energies obtained from low-field ER data.

^bNet donor concentration (remaining sample-dependent scaling factor) chosen to bring experimental mass value into agreement with theoretical mass value for $E_0 + \Delta_0$ transition.

^cRef. 15.

^dRef. 4.

^eCalculated from two-band model; see text.

that Franz-Keldysh oscillations, in the presence of two competing spectra, will be determined primarily by that component having the largest density-of-states prefactor. This is in contrast to field-induced exponential absorption edges, an effect in which light-hole bands dominate.¹⁶ The observed values of $\mu_T = 2\mu_{\parallel}/3$ for the E_1 and $E_1 + \Delta_1$ critical points are systematically lower than the only theoretical values currently available. The interband reduced mass of the E_1 critical point is slightly larger than that for $E_1 + \Delta_1$, in contrast to the predictions of the two-band model,¹⁷ for reasons which are not known. Reduced-mass values for the E_0' triplet are given only for the specific polarizations shown, since the values obtained for orthogonal polarizations were observed to be highly field dependent. This, together with the relatively large polarization anisotropies observed in the amplitudes of the main E_0' structures, suggests that the degenerate conduction and valence bands may be much more susceptible to field-induced mixing than was previously suspected.¹⁸

The large number of oscillations above the main E_2 structure indicates a well-localized origin for this spectral feature, possibly from a single set of equivalent critical points. This is particularly surprising in view of current interpretations, but is strongly supported by the fact that the measured reduced-mass value, $(0.139 \pm 0.015)m_e$, agrees quite well with the value $0.12m_e$ calculated from the two-band expression $m/\mu = 4P^2/mE_g$, where $P = 2\pi/a_0$ and a_0 is the lattice constant. The appearance of the oscillations on the high-energy side of the main structure demonstrates that μ_{\parallel} is positive, but the large polarization anisotropy of the main structure shows that at least one mass component must be negative. These results are compatible with a Σ -symmetry assignment for this transition, in agreement with possible locations predicted by band-structure calculations.

In conclusion, we have shown that reduced masses for higher-interband critical points can

be determined experimentally, thus providing a new class of parameters for band-structure analysis. The method proposed is general and may be applied to other semiconductors. Further work is in progress.

The technical assistance of A. A. Studna in the measurement of these spectra is gratefully acknowledged.

¹E. O. Kane, Phys. Rev. B 4, 1910 (1971), and 5, 1493 (1972).

²S. O. Sari, Phys. Rev. Lett. 26, 1167 (1971), and Phys. Rev. B 6, 2304 (1972).

³D. E. Aspnes and A. A. Studna, Phys. Rev. B 7, 4605 (1973).

⁴G. Dresselhaus and M. S. Dresselhaus, Phys. Rev. 160, 649 (1967).

⁵M. Welkowsky and R. Braunstein, Phys. Rev. B 5, 497 (1972).

⁶R. Cahn and M. L. Cohen, Phys. Rev. B 1, 2569 (1970).

⁷M. Cardona and F. H. Pollak, in *The Physics of Opto-Electronic Materials*, edited by W. A. Albers, Jr. (Plenum, New York, 1971), p. 81.

⁸R. R. L. Zucca and Y. R. Shen, Phys. Rev. B 1, 2668 (1970).

⁹L. V. Keldysh, Zh. Eksp. Teor. Fiz. 33, 994 (1957) [Sov. Phys. JETP 6, 763 (1958)]; W. Franz, Z. Naturforsch. 13a, 484 (1958).

¹⁰D. E. Aspnes, Phys. Rev. 147, 554 (1966), and 153, 972 (1967).

¹¹Y. Hamakawa, F. A. Germano, and P. Handler, Phys. Rev. 167, 703 (1968); T. Nishino and Y. Hamakawa, J. Phys. Soc. Jap. 26, 403 (1969).

¹²A. Frova, P. Handler, F. A. Germano, and D. E. Aspnes, Phys. Rev. 145, 575 (1966).

¹³P. Handler, S. Jasperson, and S. Koeppen, Phys. Rev. Lett. 23, 1387 (1969).

¹⁴D. E. Aspnes, Phys. Rev. Lett. 28, 913 (1972).

¹⁵P. Lawaetz, Phys. Rev. B 4, 3460 (1971).

¹⁶Yu. N. Berozashvili, A. V. Dundua, and D. Sh. Lordkipanidze, Fiz. Tverd. Tela 13, 3172 (1971) [Sov. Phys. Solid State 13, 2669 (1971)].

¹⁷M. Cardona and D. L. Greenaway, Phys. Rev. 125, 1291 (1962).

¹⁸J. E. Fischer and N. Bottka, Phys. Rev. Lett. 24, 1292 (1970).